Optical system based on time-gated, intensified charge-coupled device camera for brain imaging studies

Piotr Sawosz
Michal Kacprzak
Norbert Zolek
Polish Academy of Sciences
Institute of Biocybernetics and Biomedical Engineering
Ks. Trojdena 4
Warsaw 02-109, Poland

Wojciech Weigl
Medical University of Warsaw
Department of Anesthesiology and Intensive Care
W. Lindleya 4
Warsaw 02-005, Poland

Stanislaw Wojtkiewicz
Roman Maniewski
Adam Liebert
Polish Academy of Sciences
Institute of Biocybernetics and Biomedical Engineering
Ks. Trojdena 4
Warsaw 02-109, Poland

Abstract. An imaging system for brain oxygenation based on a time-gated, intensified charge-coupled device camera was developed. It allows one to image diffusely reflected light from an investigated medium at defined time windows delayed with respect to the laser pulse. Applying a fast optomechanical switch to deliver the light at a wavelength of 780 nm to nine source fibers allowed one to acquire images in times as short as 4 s. Thus, the system can be applied in *in vivo* studies. The system was validated in phantom experiments, in which absorbing inclusions were localized at different depths and different lateral positions. Then, the decrease in absorption of the brain tissue related to increase in oxygenation was visualized in the motor cortex area during finger tapping by a healthy volunteer. © *2010 Society of Photo-Optical Instrumentation Engineers.* [DOI: 10.1117/1.3523366]

Keywords: brain imaging; time-gated intensified charge-coupled device camera; near-infrared spectroscopy.

1 Introduction

Advanced optical techniques were proposed in the last several years for brain oxygenation assessment in animals and humans.[1] Relatively low absorption of light in tissues at near-infrared (NIR) wavelengths allows for light penetration in depths of 1–2 cm into the body[2] and makes it possible to assess tissue absorption by analysis of the intensity of reemitted light. NIR spectroscopy (NIRS), which is based on the differences in spectral properties of oxy- and deoxyhemoglobin in the NIR wavelength region,[3,4] showed its usefulness in brain oxygenation studies carried out in newborns[5] and adults.[6] This technique was validated in neurophysiological studies[7] as well as in clinical measurements.[8,9] It was also reported that brain perfusion can be assessed in NIR wavelength range by analysis of inflow and washout of an optical contrast agent.[10–12]

Many authors showed that the optical signals measured on the surface of the head depend on brain-tissue oxygenation as well as oxygen saturation of extracerebral tissues (skin, skull, etc.). Different source-detector separations as well as light-detection principles were utilized in order to measure signals related to absorption changes appearing in the brain cortex and to avoid influence of contaminating signals originating from changes in extracerebral tissues. Particularly, it was shown that an increase in interoptode distance leads to an increase in the measurement sensitivity to the absorption changes in the brain.[13–15] It was also reported that utilization of the frequency-domain technique[16] as well as time-resolved measurements[17–19] allow one to discriminate information originating from the cortex and extracerebral tissues.

In all proposed optical setups, a limited number of source-detector pairs distributed on the surface of the head was applied with relatively large source-detector separations. However, this solution leads to problems connected with coupling of light into the tissue and fixing fibers or fiber bundles on the tissue of interest.

The intensified charge-coupled device (ICCD) camera was tested in time-resolved photon migration studies carried out in transmission geometry.[20] Recently, the ICCD was applied in a brain imaging system[21] in which the camera was utilized as a large time-resolved detector. Furthermore, the camera was used for imaging the surface of the head illuminated by multiple sources.[22]

The ICCD camera can be potentially used for imaging a large area of a tissue in transmission or reflectance geometry and allows for acquisition of photons remitted from the tissue, simultaneously, at different source-detector separations. Simultaneous acquisition of data at multiple detection spots may allow one to improve spatial resolution. Finally, utilization of a time-gating principle leads, potentially, to improved discrimination of depth at which absorption changes appear.

In this paper, we present a brain imaging system based on a time-gated ICCD camera. The system was validated in phantom experiments, and its ability to provide depth-discrimination imaging is shown. Furthermore, the high speed of data acquisition allowed for application of the setup in *in vivo* studies carried out during functional brain cortex stimulation.

Address all correspondence to: Piotr Sawosz, Polish Academy of Sciences, Institute of Biocybernetics and Biomedical Engineering, Ks. Trojdena 4, 02-109 Warsaw, Poland; Tel: 48-22-659-91-43, ext. 113; Fax: 48-22-659-70-30; E-mail:psawosz@ibib.waw.pl
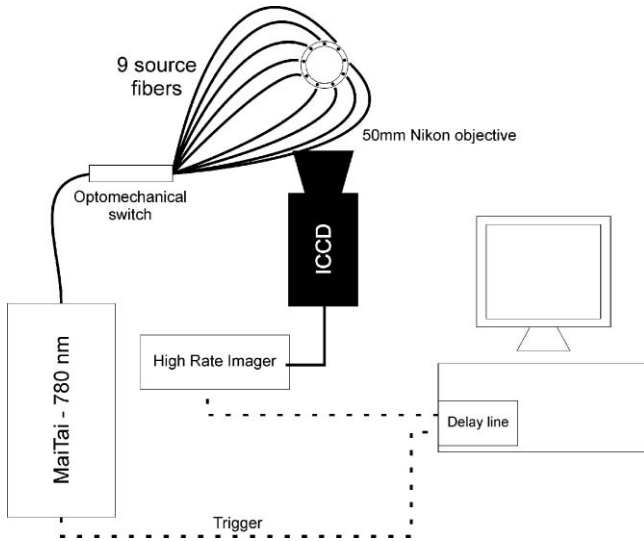
Fig. 1 Setup of the imaging system. MaiTai—Ti:sapphire pulsed laser source, ICCD—time-gated, intensified CCD camera.

2 Methods and Instrumentation

2.1 Setup of ICCD Camera-Based Imaging System

The imaging system (Fig. 1) allows for measurement of diffusely reflected light from a tissue in reflectance geometry. The tips of nine emitting fibers of a diameter of 200 μm (NA = 0.22) are located on the ring of a diameter of 5 cm around the imaged area. The fibers are independently spring mounted; therefore, they can be easily located on the rough structure of a human head (see Fig. 2).

The fibers were used to deliver femtosecond laser pulses ([full width at half maximum FWHM < 100 fs]) generated by MaiTai laser (SpectraPhysics, Irvine CA, USA) to the studied object

Fig. 2 Emitting fibers located on the ring, spring mounted independently.
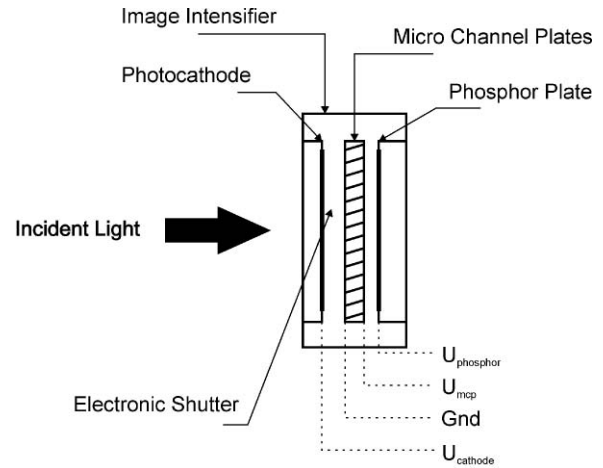
Fig. 3 Scheme of the image intensifier with electronic shutter.

(phantom or tissue). The laser was tuned to a wavelength of 780 nm. The wavelength was selected considering our previous studies carried out with indocyanine green as a contrast agent.[23] It should be noted that because of using only one wavelength, the measurement does not allow for estimation of changes in concentrations of oxy- and deoxyhemoglobin. However, the measured signals are sensitive to changes in oxygenation because the chosen wavelength did not match with isosbestic point.[24] Additionally, the availability of stable laser pulses was considered together with the optimal sensitivity of the ICCD camera. The laser operated at an 80-MHz repetition rate, however the delay line DEL350 (Becker&Hickl, Berlin, Germany) was limited to 40 MHz; thus, the system was triggered with every second laser pulse. One of two standard MaiTai trigger outputs, electronically divided into 40 MHz was used. The power of the laser was 0.85 W; however, power at the tips of the fibers was limited to 20 mW. During the measurements, the source position was sequentially switched between nine locations on the phantom or tissue using a fast optomechanical switch (Piezosystem Jena, Jena, Germany) with switching time of <5 ms. For each position of the source, images of diffusely reflected light were recorded using time-gated ICCD camera (PicoStar HR, LaVision, Goettingen, Germany). The measured FWHM of the instrumental response function (IRF) of the setup is ~350 ps. The IRF includes dispersion of light in the emitting fibers, jitters of the electronics, and width of the time window of the camera. This width of IRF is better than reported by Selb *et al.* in a similar optical setup,[25] but it also does not diverge significantly from time-resolved brain-monitoring systems reported by various authors.[26–28]

The camera is equipped with an image intensifier containing a microchannel plate (MCP) and electronic shutter between the photocathode and the MCP (Fig. 3). During the whole experiment, a high potential at the MCP is applied. Time gating is realized by electronic shutter and high-rate imager (Kentech Instruments Ltd., Wallingford, UK). The camera collects diffusely reflected photons within a 200-ps-long time window at defined delays in respect to the laser pulse. Late time windows are of special interest because the photons collected at these time windows have higher probability of penetrating into deeper tissue compartments. Because the number of photons collected at late time windows is low, a high gain on MCP must be applied.
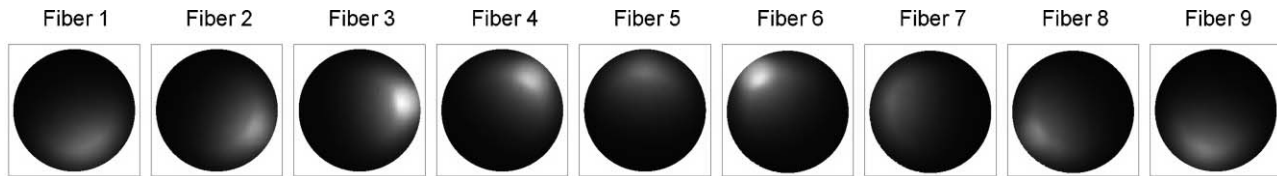
| Fiber 1 | Fiber 2 | Fiber 3 | Fiber 4 | Fiber 5 | Fiber 6 | Fiber 7 | Fiber 8 | Fiber 9 |

Fig. 4 Images of diffusely reflected light obtained for each of nine emitting fibers located on a ring surrounding imaged area.

However, the massive number of early photons arriving at early time windows should not be detected.

The key element of the ICCD camera is the electronic shutter, which provides acceleration of the electrons from the photocathode into the MCP only when the trigger is applied (when the potential between $U_{cathode}$ and *Gnd* is negative). Therefore, one can "filter" a dangerously high number of early photons and amplify only late ones. Thus, the measurement procedure does not lead to damage of the MCP. However, it should be noted that the photocathode is deteriorated during the experiment and the large number of early photons must be converted to electrons, which limits the lifetime of the photocathode.

2.2 Instrument Calibration

In the optomechanical switch (Fig. 1), different optical pathlengths for each emitting fiber were observed. This phenomenon was very critical, especially considering the measurements for a defined time window. It was necessary to provide that time windows for different emitting fibers were defined at exactly the same temporal position in respect to the laser pulse. Therefore, the calibration of the optomechanical switch was necessary.

We measured IRF for each of the emitting fibers and evaluated the temporal position of the maximum of probability. Thus, the time delays characterizing selected fibers were obtained. They varied up to 0.9 ns. The controlling software was enhanced by adding a calibration procedure based on adjustments of the delay line for every fiber separately. During changes of the switch position, the delay is changed according to an obtained calibration matrix containing measured temporal delays in order to adjust the position of the time window.

Relatively low dynamic range of the ICCD causes that the acquisition time needs to be adjusted for different delays of time windows with respect to the laser pulse. In order to achieve high signal-to-noise ratio it is impossible to measure different time windows at the same photon collection time. Images for the whole measured time range for a homogenous medium with optical properties similar to these that can be obtained in human tissue were acquired. For each time window, the number of photons was calculated. These numbers of photons acquired at

different time windows were used for determination of acquisition time for different time windows.

2.3 Image Acquisition and Processing

The measurement was controlled with in-house software developed in the DaVis environment (LaVision, Germany). The software controls the whole process of image acquisition: defining parameters of the acquisition, defining the time window's position with the use of a delay line, and controlling the process of switching the positions of the source. To control the optomechanical switch, the script, written in C + +, must have been executed in DaVis, which allowed us to send switching commands via the Line Print Terminal (LPT) port. Images are collected with a resolution of 640 × 480 pixels and stored on the hard disk of a PC in 12-bit RAW format. The CCD's pixel size on the sample is ~0.15 mm.

As shown in Fig. 4, images of light diffusely reflected from the phantom were collected for each of nine emitting fibers. Sequential switching of the laser light to the single source positions was carried out, and corresponding images of the area inside the ring formed by source fibers were acquired at defined time window. In the physical phantom, studies for each position of the emitting fiber of the background image was subtracted (see Fig. 5). The background images were obtained during measurement carried out in a homogenous medium. Images obtained for each of nine source positions were summed up. Resulting images were normalized from 0 to 256 against the minimum and maximum number of photons of images obtained at a certain delay of time window.

2.4 Phantom Experiments

The plexiglas aquarium with a front side made of 50-μm thick Mylar film (DuPont Polska, Warsaw, Poland) was used. It was filled with water, milk, and ink solution (3:1 water to milk with fat content of 3.2%) of the optical properties $\mu_a = 0.12$ cm^{-1} and $\mu'_s = 15$ cm^{-1}. Absorbing inclusions located at various positions in the phantom were applied in order to show depth-discrimination of the time-gated measurements. Small balls (6 mm diam) made of gelatin were used as absorbing
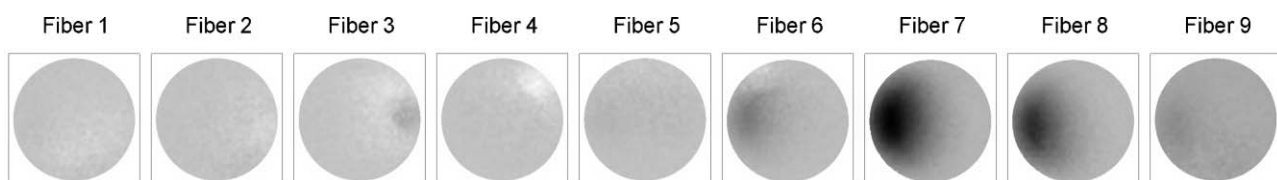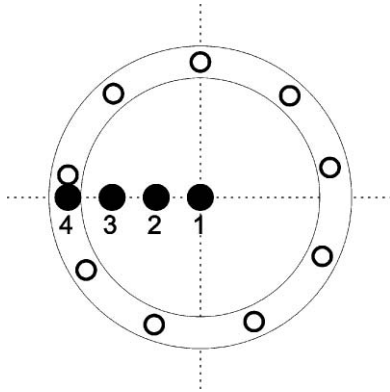
| Fiber 1 | Fiber 2 | Fiber 3 | Fiber 4 | Fiber 5 | Fiber 6 | Fiber 7 | Fiber 8 | Fiber 9 |

Fig. 5 Images of diffusely reflected light for nine emitting fibers after background subtraction. Black spot correspondes to an increase in absorption in a place of absorbing inclusion.

Fig. 6 Positions of inclusion with respect to the imaging area (black circles). Fiber positions are marked with black rings.

inclusions. The balls were manufactured of mixture of 30 g of gelatin with 400 ml of milk, water, and ink solution by filling a homemade metallic form. Inclusions were fixed in the phantom with the use of a transparent fishing line (thickness, 0.2 mm). The inclusions were fixed at four different lateral positions (Fig. 6) and five different depths from $d = 8$ to $d = 20$ mm. The absorption coefficient of the inclusion was ~50 times higher than the absorption coefficient of the surrounding medium. The differences in ink concentrations were similar to the ones reported by Selb et al..[25] Measurements for three different time windows delayed in respect to the maximum of the IRF were carried out.

2.5 In Vivo Measurements

A series of measurements during sensomotoric cortex stimulation were carried out. The monitoring during left-hand finger-tapping stimulation was performed on two volunteers, 30 and 27 years old. They were instructed to touch their thumb with their index and middle fingers, self-controlled, with frequency of ~3 Hz. The measurements were carried out in sitting position. The optode setup was positioned on the right side of the head in such a way that its center was located on the C4 position (according to the 10–20 EEG standard[29]). The stimulation procedure consisted of five cycles of 30-s finger tapping, followed by 30 s of rest. The surface of the tissue was imaged at a single time window delayed by 2 ns with respect to the maximum of the IRF. Acquisition of nine images for all source positions, resulting in single integrated image of distribution of reflectance at defined time window took ~4 s. The resulting image was smoothed with the use of a 2-D digital filter under MATLAB environment.

3 Results

3.1 Phantom Measurements

The absorbing inclusion was located at 20 different positions in the homogeneous liquid phantom. For each position of the inclusion, the scanning procedure was performed in order to obtain images for three time windows delayed by 1.5, 2.5, and 3.5 ns with respect to the maximum of the IRF.

In Fig. 7, integrated images of absorbing inclusion positioned at different depths are presented. It can be observed that the
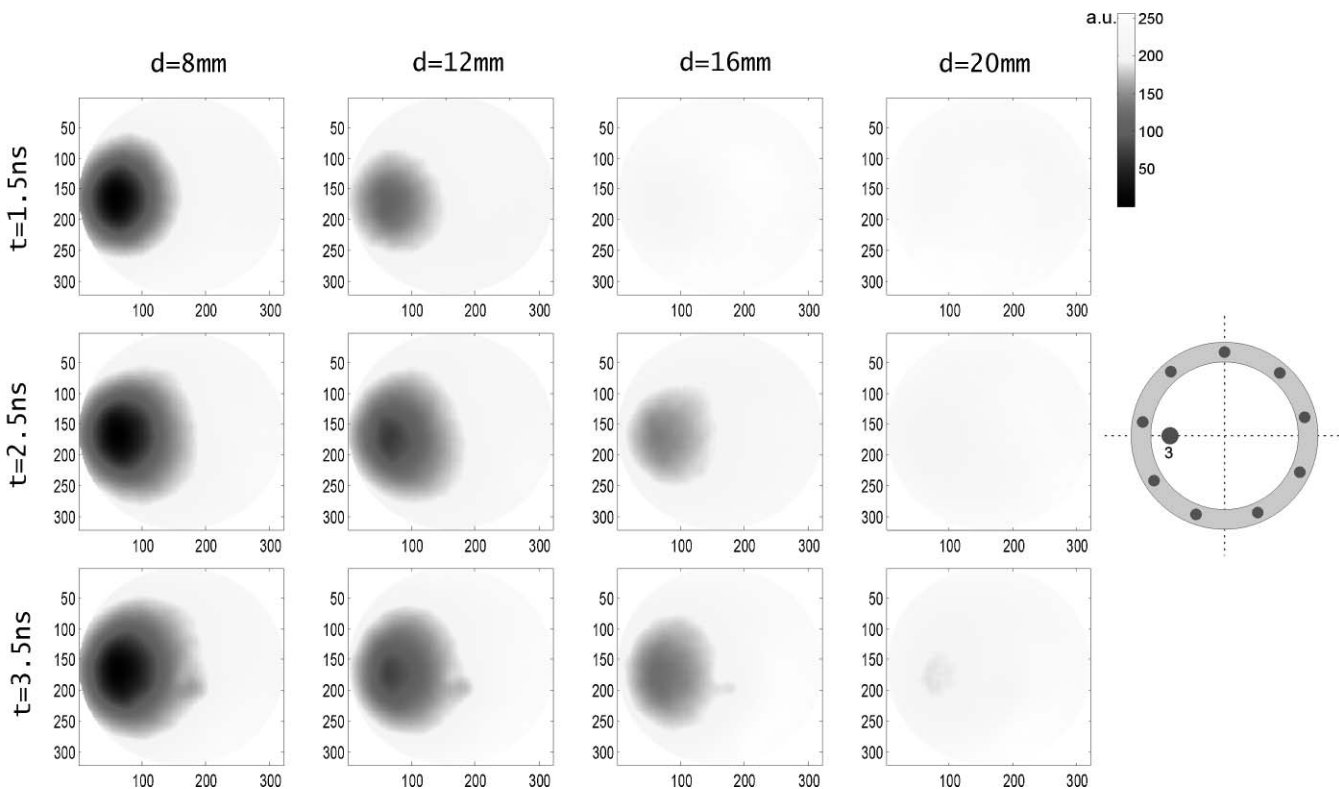
Fig. 7 Integrated images of diffusely reflected light obtained by summing up the images recorded for each of nine source positions. Images were obtained for inclusion located at four different depths end for three different time windows delayed by 1.5, 2.5, and 3.5 ns, respectively, to the maximum of the IRF.
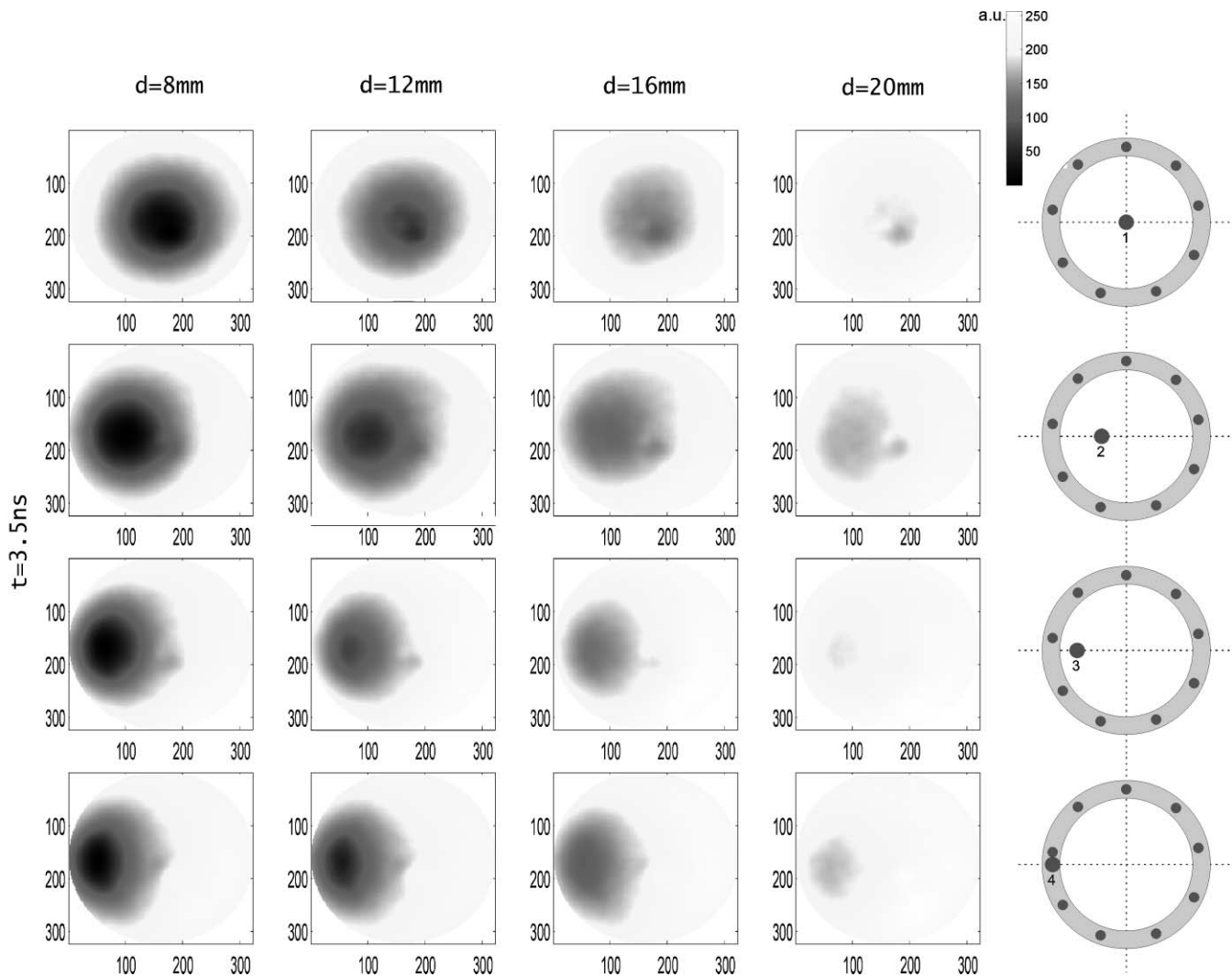
Fig. 8 Images of diffusely reflected light recorded for single time window delayed by 3.5 ns with respect to the maximum of the IRF. The images were obtained for absorbing inclusion located at various depths and different lateral positions.

local increase in the number of absorbed photons at a selected position of inclusion depends on the time window. Effective detection of the inclusion positioned deeper is possible only for later time windows. Inclusion positioned at a depth of 20 mm was not detected for the first (earliest) time window. It can also be noted that for early time window, the image of the inclusion is smaller than the same inclusion imaged for longer delays. This effect can be explained by the higher number of scattering events corresponding to the longer time of flight of the photons. Thus, the higher probability of lateral penetration of the photons can be noted. These results suggest that analysis of delayed time windows allow for selective evaluation of absorption changes located deeply in the medium.

In Fig. 8, results of imaging of the absorbing inclusion, positioned at different depths and different lateral positions, are presented. These images were obtained for a single time window delayed by 3.5 ns in respect to the maximum of the IRF. It can be observed that inclusion can be localized at all lateral positions. However, the shapes and sizes of the images of absorbing inclusions are different. The shape of the image of the

inclusion is most regular when the inclusion is located in the center of the imaged area.

3.2 *In Vivo Measurements*

In Fig. 9, spatial distribution of changes in the number of photons detected in the motor cortex area during the finger-tapping procedure is presented. As mentioned earlier, we performed five cycles of the 30-s stimulation period, followed by 30 s of rest. In the first step of analysis, we averaged all images obtained for stimulation periods and all images obtained for rest periods. As a result, two images were obtained, one corresponding to the stimulation period and one corresponding to the rest period. Furthermore, the rest image was subtracted from the stimulation image (see Fig. 9). Zero value represents the mean number of photons during the experiment. An increase in the number of photons at a wavelength of 780 nm during stimulation can be observed. This increase is connected with the decrease in tissue absorption caused by an increase in brain tissue oxygenation. The
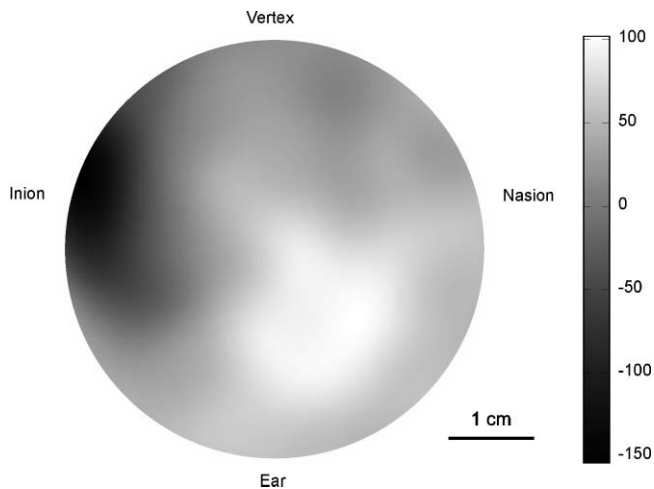
Fig. 9 Image representing a decrease in absorption in motor cortex caused by finger-tapping stimulation. The directions to the Nasion, Ear, Inion, and Vertex on human head are indicated. Middle of the image corresponds to the position of C4 point of 10–20 EEG system.

stimulated area can be observed in the lower-right quadrant of the image.

4 Discussion and Conclusions

Construction of the imaging system, based on an ICCD camera optimized for brain oxygenation studies was presented. The system was validated in phantom experiments and in first preliminary *in-vivo* measurements. In experiments carried out with the use of the an homogeneous medium with absorbing inclusion, the technique of localization of changes of absorption at different depths (up to 20 mm) was validated. Also, dependence of sensitivity of the setup on the lateral position of the absorbing inclusion was shown.

In vivo measurements were carried out during a finger-tapping experiment on two volunteers. Influence of sensomotoric stimulation on the oxygenation of motor cortex was observed. A decrease in absorption corresponding with an increase in oxyhemoglobin concentration was noted. This effect is connected with an increased demand of oxygen caused by intensive neural activation in motor cortex area.[30] Results of our measurements are in line with the data reported by other authors using various techniques. A decrease in deoxyhemoglobin concentrations, stimulated by a finger-tapping procedure was reported before in many studies carried out by functional magnetic resonance imaging.[31] These effects were also observed with the use of optical methods based on continuous-wave NIRS[32] as well as frequency-modulated NIRS instruments[33] and methods utilizing measurement of photon times of flight.[17,34]

The studies carried out by Selb *et al.*[25] were based on fast data acquisition from multiple time windows with the use of an ICCD time-gated system and source fibers of different lengths. However, in that proposal, the ICCD camera was used as a multichannel time-resolved detector rather than an imaging tool.

Our setup represents improvement in the proposition reported by Sase *et al.*[22] The setup proposed in that report was rather slow and allowed only for presentation of its usefulness in phantom experiments. In our setup, the fast optomechanical switch was applied for sequential switching of the source position, which allowed one to reduce the time of acquisition of the single image. Finally, the single-image acquisition time on the order of a few seconds was reached, which is much shorter than the time in our previous setup based on slow scanning of the object of interest.[35,36] This time is short enough for monitoring the absorption changes at a single wavelength and a for single time window. This solution allowed us to show feasibility of depth discrimination with the application of the time-gated ICCD setup and to apply this construction in *in vivo* studies. Results of our experiments show that the ICCD-based time-gated detection allows us to visualize changes in absorption of the tissue during sensimotor cortex stimulation. However, it should be noted that the proposed method does not allow for assessment of hemoglobin concentration because the system operates only at a single wavelength. Potentially, the proposed method can be used with application of more laser light sources. Application of a delay between pulses obtained from two light sources of different wavelengths would allow one to analyze time windows corresponding to these two wavelengths. However, such a procedure will lead to an increase in time needed to acquire images. Considering that the time resolution of the data acquisition is already quite critical from the point of view of the motor-stimulation paradigm (4 s needed for collection of single image), this scenario seems to be unrealistic. In functional imaging studies or contrast-agent bolus monitoring, acquisition time is a critical parameter because the measurement must follow fast physiological effects or inflow and washout of the dye. On the other hand, from an instrumental point of view, the acquisition time strongly depends on the number of wavelengths applied and number of monitored time windows. Shortening of the acquisition time for single-source position leads also to a decrease in signal-to-noise ratio.

The proposed brain imaging system with optomechanical switch may be further modified in order to shorten the acquisition time. It should be considered to image diffusely reflected light for a combination of multiple-length fiber sources at the same time, which may allow one to obtain images for two or more time windows.

It should be also noted that the imager is quite difficult to apply in a human head because of light-coupling problems in the source positions. An additional problem is light scattering in the imaged area caused by the presence of hair. This effect is not as critical for a subject with short hair of constant length in the whole imaged area. In such a case, the hair can be treated as a scattering filter in front of the detector, which limits spatial resolution of the setup.

References

1. E. M. Hillman, "Optical brain imaging *in vivo:* techniques and applications from animal to man," *J. Biomed. Opt.* **12**(5), 051402 (2007).

2. F. F. Jobsis, "Noninvasive, infrared monitoring of cerebral and myocardial oxygen sufficiency and circulatory parameters," *Science* **198**(4323), 1264–1267 (1977).

3. S. Wray, M. Cope, D. T. Delpy, J. S. Wyatt, and E. O. Reynolds, "Characterization of the near infrared absorption spectra of cytochrome aa3 and haemoglobin for the non-invasive monitoring of cerebral oxygenation," *Biochim. Biophys. Acta* **933**(1), 184–192 (1988).

4. M. Cope, D. T. Delpy, E. O. Reynolds, S. Wray, J. Wyatt and P. van der Zee, "Methods of quantitating cerebral near infrared spectroscopy data," *Adv. Exp. Med. Biol.* **222**, 183–189 (1988).

5. K. Sakatani, S. Chen, W. Lichty, H. Zuo, and Y. P. Wang, "Cerebral blood oxygenation changes induced by auditory stimulation in newborn infants measured by near infrared spectroscopy," *Early Hum. Dev.* **55**(3), 229–236 (1999).

6. H. Obrig and A. Villringer, "Beyond the visible—imaging the human brain with light," *J. Cereb. Blood Flow Metab.* **23**(1), 1–18 (2003).

7. A. Villringer and B. Chance, "Non-invasive optical spectroscopy and imaging of human brain function," *Trends Neurosci.* **20**(10), 435–442 (1997).

8. M. Wolf, M. Ferrari, and V. Quaresima, "Progress of near-infrared spectroscopy and topography for brain and muscle clinical applications," *J. Biomed. Opt.* **12**(6), 062104 (2007).

9. M. Kacprzak, A. Liebert, P. Sawosz, R. Maniewski, G. Madycki, and W. Staszkewicz, "Intraoperative monitoring of the cerebral oxygenation during carotid endarterectomy using time-resolved brain imager," presented at ECBO 2009, Munich (2009).

10. E. Keller, A. Nadler, H. Alkadhi, S. S. Kollias, Y. Yonekawa, and P. Niederer, "Noninvasive measurement of regional cerebral blood flow and regional cerebral blood volume by near-infrared spectroscopy and indocyanine green dye dilution," *Neuroimage* **20**(2), 828–839 (2003).

11. A. Liebert, H. Wabnitz, J. Steinbrink, M. Moller, R. Macdonald, H. Rinneberg, A. Villringer, and H. Obrig, "Bed-side assessment of cerebral perfusion in stroke patients based on optical monitoring of a dye bolus by time-resolved diffuse reflectance," *Neuroimage* **24**(2), 426–435 (2005).

12. C. Terborg, S. Bramer, S. Harscher, M. Simon, and O. W. Witte, "Bedside assessment of cerebral perfusion reductions in patients with acute ischaemic stroke by near-infrared spectroscopy and indocyanine green," *J. Neurol. Neurosurg Psychiatry* **75**(1), 38–42 (2004).

13. T. J. Germon, P. D. Evans, A. R. Manara, N. J. Barnett, P. Wall, and R. J. Nelson, "Sensitivity of near infrared spectroscopy to cerebral and extra-cerebral oxygenation changes is determined by emitter-detector separation," *J. Clin. Monit. Comput.* **14**(5), 353–360 (1998).

14. M. A. Franceschini, S. Fantini, L. A. Paunescu, J. S. Maier, and E. Gratton, "Influence of a superficial layer in the quantitative spectroscopic study of strongly scattering media," *Appl. Opt.* **37**(31), 7447–7458 (1998).

15. J. Steinbrink, H. Wabnitz, H. Obrig, A. Villringer, and H. Rinneberg, "Determining changes in NIR absorption using a layered model of the human head," *Phys. Med. Biol.* **46**(3), 879–896 (2001).

16. M. A. Franceschini, S. Thaker, G. Themelis, K. K. Krishnamoorthy, H. Bortfeld, S. G. Diamond, D. A. Boas, K. Arvin, and P. E. Grant, "Assessment of infant brain development with frequency-domain near-infrared spectroscopy," *Pediatr Res* **61**(5 Pt 1), 546–551 (2007).

17. H. Wabnitz, M. Möller, A. Liebert, H. Obrig, J. Steinbrink, and R. Macdonald, "Time-Resolved Near-Infrared Spectroscopy and Imaging of the Adult Human Brain," *Advances in Experimental Medicine and Biology* **662**, 143–148 (2010).

18. L. Gagnon, C. Gauthier, R. D. Hoge, F. Lesage, J. Selb, and D. A. Boas, "Double-layer estimation of intra- and extracerebral hemoglobin concentration with a time-resolved system," *J. Biomed. Opt.* **13**(5), 054019 (2008).

19. A. Liebert, H. Wabnitz, J. Steinbrink, H. Obrig, M. Moller, R. Macdonald, A. Villringer, and H. Rinneberg, "Time-resolved multidistance near-infrared spectroscopy of the adult head: intracerebral and extracerebral absorption changes from moments of distribution of times of flight of photons," *Appl. Opt.* **43**(15), 3037–3047 (2004).

20. C. D'Andrea, D. Comelli, A. Pifferi, A. Torricelli, G. Valentini, and R. Cubeddu, "Time-resolved optical imaging through turbid media using a fast data acquisition system based on a gated CCD camera," *J. Phys. D* **36**(14), 1675–1681 (2003).

21. J. Selb, J. J. Stott, M. A. Franceschini, A. G. Sorensen, and D. A. Boas, "Improved sensitivity to cerebral hemodynamics during brain activation with a time-gated optical system: analytical model and experimental validation," *J. Biomed. Opt.* **10**(1), 11013 (2005).

22. I. Sase, A. Takatsuki, J. Seki, T. Yanagida, and A. Seiyama, "Non-contact backscatter-mode near-infrared time-resolved imaging system: preliminary study for functional brain mapping," *J. Biomed. Opt.* **11**(5), 054006 (2006).

23. M. Kacprzak, A. Liebert, P. Sawosz, N. Zolek, and R. Maniewski, "Time-resolved imaging of fluorescent inclusions in optically turbid medium—phantom study," *Opto-Electron. Rev.* **18**(1), 37–47 (2010).

24. M. Cope, "The application of near infrared spectroscopy to non invasive monitoring of cerebral oxygenation in the newborn infant," PhD Thesis, Department of Medical Physics and Bioengineering, University College London, London (1991).

25. J. Selb, D. K. Joseph, and D. A. Boas, "Time-gated optical system for depth-resolved functional brain imaging," *J. Biomed. Opt.* **11**(4), 044008 (2006).

26. D. Contini, A. Torricelli, A. Pifferi, L. Spinelli, F. Paglia, and R. Cubeddu, "Multi-channel time-resolved system for functional near infrared spectroscopy," *Opt. Express.* **14**(12), 5418–5432 (2006).

27. M. Kacprzak, A. Liebert, P. Sawosz, N. Zolek, and R. Maniewski, "Time-resolved optical imager for assessment of cerebral oxygenation," *J. Biomed. Opt.* **12**, 034019 (2007).

28. H. Wabnitz, M. Moeller, A. Liebert, H. Obrig, J. Steinbrink, and R. Macdonald, "Time-resolved near-infrared spectroscopy and imaging of the adult human brain," *Adv. Exp. Med. Biol.* **662**, 143–148 (2010).

29. G. H. Klem, H. O. Luders, H. H. Jasper, and C. Elger, "The ten-twenty electrode system of the International Federation. The International Federation of Clinical Neurophysiology," *Electroencephalogr. Clin. Neurophysiol. Suppl.* **52**, 3–6 (1999)

30. C. G. Santosh, J. E. Rimmington, and J. J. Best, "Functional magnetic resonance imaging at 1 T: motor cortex, supplementary motor area and visual cortex activation," *Br. J. Radiol.* **68**(808), 369–374 (1995).

31. E. M. Wassermann, B. Wang, T. A. Zeffiro, N. Sadato, A. Pascual-Leone, C. Toro, and M. Hallett, "Locating the motor cortex on the MRI with transcranial magnetic stimulation and PET," *Neuroimage* **3**(1), 1–9 (1996).

32. B. W. Zeff, B. R. White, H. Dehghani, B. L. Schlaggar, and J. P. Culver, "Retinotopic mapping of adult human visual cortex with high-density diffuse optical tomography," *Proc. Natl. Acad. Sci. USA* **104**(29), 12169–12174 (2007).

33. M. Wolf, U. Wolf, V. Toronov, A. Michalos, L. A. Paunescu, J. H. Choi, and E. Gratton, "Different time evolution of oxyhemoglobin and deoxyhemoglobin concentration changes in the visual and motor cortices during functional stimulation: a near-infrared spectroscopy study," *Neuroimage* **16**(3 Pt 1), 704–712 (2002).

34. T. Sander, A. Liebert, M. Burghoff, H. Wabnitz, R. Macdonald, and L. Trahms, "DC-magnetoencephalography and time-resolved near-infrared spectroscopy combined to study neuronal and vascular brain responses," *Physiological Measurement* **28**, 651–664 (2007).

35. P. Sawosz, M. Kacprzak, A. Liebert, and R. Maniewski, "Application of time-gated, intensified CCD camera for imaging of absorption changes in non-homogeneous medium," in IFMBE Proceedings, Vol. 16 Eds. T. Jarm, P. Kremer, A. Zupanic, 11th Mediterranean Conf. on Medical and Biological Engineering and Computing, Lubljana, Slovenia, Springer, Berlin Heidelberg, New York (2007).

36. P. Sawosz, M. Kacprzak, A. Liebert, and R. Maniewski, "Time-gated, intensified CCD camera for imaging of a non-homogenous medium at null source-detector separation," presented at European Conf. on Biomedical Optics, Munich (2007).